Journal of Aeronautical and Automotive Engineering (JAAE)
p-ISSN: 2393-8579; e-ISSN: 2393-8587; Volume 3, Issue 2; April-June, 2016 pp. 43-48

http://www.krishisanskriti.org/Publication.html

Vortex Control by a Vertical Splitter Plate Placed Upstream of a Square Cylinder in non-Newtonian Flow

Nidhi[1], Sudipto Sarkar[2] and Anamika Paul[3]

[1]Graduate Student, School of Chemical Engineering, Galgotias University, India
[2]School of Mechanical Engineering, Galgotias University, India
[3]School of Chemical Engineering, Galgotias University, India
E-mail: [2]sudipto.sarkar@galgotiasuniversity.edu.in

Abstract—*In the present research work simulation of non-Newtonian fluid flow is carried out for vortex control of a square cylinder with a vertical upstream splitter plate. The unsteady two-dimensional Navier-Stokes equations (momentum and continuity equations) are solved using Ansys Fluent. Six different cases have been considered by varying the gap-ratio (G/a = 2.5 and 3, where 'G' is the gap between cylinder and plate and 'a' is the length of the side of the cylinder) and three different flow behavior indices (n = 0.8, 1 and 1.2). Changes in flow structures have been reported when the fluid flow is non-Newtonian and also the mean aerodynamic forces differ from Newtonian fluid flow.*

1. INTRODUCTION

The present paper deals with the understanding of rheology of fluid and analysis of fluid flow phenomena, using the CFD simulation software Ansys Fluent. Rheology of fluid is the classification of fluid group considering the Newton's law of viscosity. The fluid obeying this law are called Newtonian and the rest of them are known as non-Newtonian fluids. They are further classified based on their dependency on time, temperature changes, etc. The maximum number of fluids available in nature and/or artificially made from industrial applications is non-Newtonian in nature. Considering the availability of non-Newtonian fluids in the environment (or artificially made), control of the vortices of bluff bodies by passive means was simulated in the present work.

Bluff bodies are characterized usually by a huge unsteady downstream wake region that leads to considerable fluctuating fluid forces. The wake and the separated flow region can be reduced by the flow control which, in turn, reduces unsteadiness and the forces on the object. The flow control methods used to suppress the aerodynamic forces can be classified into two categories:

1. Active control methods in which the flow is controlled by supplying external energy by means of forced fluctuations and jet blowing [1].

2. Passive control methods in which the flow is controlled by modifying the shape of the body or by attaching additive devices such as control rod, plate or roughness elements onto the body [2].

In the last few decades, research in the field of passive steady flow control has shown that a splitter plate set along the bluff body wake centerline reduces drag and may inhibit vortex shedding [3-6]. Malekzadeh and Sohankar [7] investigated the flow over cylinder and upstream control plate. The thickness of the plate varied from 0.1*D* to 0.9*D* and the gap between the cylinder and plate varied from 1.1*D* - 7*D* in between *Re* = 50 to 200. Three major regimes were observed in their work. In first and second regimes vortex shedding from control plate is suppressed, but in third regime, vortex formed behind the cylinder and plate. Also in the regime II, significant reduction of fluid forces is observed with a sudden increase in drag. Additionally, lift values is observed at critical distance for all control plate width. This drastic change is associated with the change in flow pattern from regime II to III and beginning of vortex shedding from control plate. They reported the reduction of time averaged drag coefficient of square cylinder with increase in *Re* and that the maximum reduction in aerodynamic forces was observed at *Re* = 200.

Numerical simulation of unbounded creeping flow of dilute polymer solutions past cylinders and spheres using a suspension of dumbbells model with finite extensibility were performed by Chilcott and Rallison [8]. It was observed that the drag coefficient variation with the Weissenberg number for the flow past a sphere first decreases slightly, and then increases for all model parameters.

Kato and Mizuno [9] measured the drag force in the *Re* range of 1×10^4–5×10^4 for the flow past a cylinder with and without polymer. They found that drag forces in the *Re* range of 1–100 are barely affected by the polymers. Important drag reduction was found in the *Re* range of 10^3–5×10^4 for the polymer

solution. The maximum drag reduction is barely affected by the Reynolds number in the range of $Re > 8 \times 10^3$.

From these literature reviews it can be concluded that almost all studies in controlling of vortex shedding using splitter plate have been carried out considering Newtonian flow environment. However, in process industries and chemical industries a huge number of fluids are used which are non-Newtonian in nature. Keeping this in view, in the present work authors simulate the wake-control problem considering the nature of the fluid as pseudoplastic (n < 1) and dilatant (n > 1). Subsequently, the differences in downstream flow field of these types of fluid with respect to Newtonian flow (n = 1) field are reported.

2. NUMERICAL METHODS

2.1 Governing Equations

Depending on Newton's law of viscosity, fluids are classified as Newtonian (following the Newton's law) and non-Newtonian (not following Newton's law). Further non-Newtonian fluids in which rheological behavior depend only on the shear stress (at constant temperature) are considered as time-independent. The shear stress τ of these kind of fluids can be expressed in power-law form $\tau = K\left(\frac{\partial u}{\partial y}\right)^n$, where K is the flow consistency index and $\frac{\partial u}{\partial y}$ is the velocity gradient perpendicular to the plane of shear. The generalized Navier-Stokes equations are used for momentum considering the shear stress obtained from above equation.

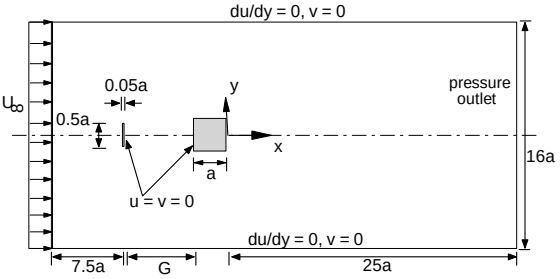

Fig. 1: Schematic diagram of flow geometry along with boundary conditions

2.2 Computational details

The entire work is divided in three parts and the following softwares are used to calculate or interpret results from each part:

a) Gambit 2.2.30 is used for Pre-processing, i.e., for developing the flow domain and to impose the boundary conditions.

b) Fluent 14.5 is used as a solver, i.e., to solve the 2-D Navier-Stokes equations (momentum) numerically.

c) Tecplot 8 is used as post processor.

The schematic diagram of flow geometry along with the boundary conditions is shown in Fig. 1 for a better understanding of the present problem. The co-ordinates x and y denote the streamwise and flow-normal directions respectively and the corresponding velocities are denoted by u and v. The origin of the axes lies at the centre of the downstream face of the cylinder. Here the boundary conditions are set by considering velocity inlet ($u = U_\infty$), pressure outlet, symmetry (free-slip boundary condition) at upper and lower domain. Wall boundary condition ($u = v = 0$) is imposed both on the cylinder and the splitter plate surfaces. Since the flow is purely one dimensional, hence flow exists only in x direction, where velocity inlet boundary condition is used to define the flow velocity at the inlet, i.e., $u = 1$, $v = 0$.

The flow-domain consists of square cylinder and vertical splitter plate such that the plate is placed vertically with respect to flow and its length is half of side of the cylinder. Also the body centers of both the geometry pass through the same centerline. Six different cases are considered by varying the gap between the cylinder and the plate (G/a = 2.5, 3) and the power index number (n = 0.8, 1, 1.2). Change in flow behavior is observed due to various gap ratios as well as different type of fluids (both Newtonian and non-Newtonian).

A total of 297 × 208 grid points are employed for G/a = 3 after the grid independence study. In detail, a total of 101 × 80 uniform grid points are employed in a domain (size 5.05a × 2a) covering both the square cylinder and the splitter plate. Away from this box, grid points are slowly stretched out in all directions. The number of grid points in the streamwise direction for G/a = 2.5 and 3.5 are 287 and 307 respectively, although no change has been made in the flow normal direction.

The Navier-Stokes (momentum) equation is then non-dimensionalized by considering a and U_∞ as unity. The flow field is then solved by Ansys Fluent 14.5 using SIMPLE algorithm in second-order upwind momentum scheme with a standard pressure solver. A total of 20 iterations at each time step are considered to increase the accuracy of the solution.

3. RESULTS AND DISCUSSION

To understand the effect of non-Newtonian fluid flow on splitter plate cylinder pair, simulation is carried out at n = 0.8, 1 and 1.2. Figures 2-7 represent the instantaneous flow field for all 6 cases considering 5 different flow variables, namely, spanwise vorticity (ω_z), streamwise velocity (u), flow normal velocity (v), coefficient of pressure ($C_p = \frac{P-P_\infty}{\frac{1}{2}\rho U_\infty^2}$) and streamlines.

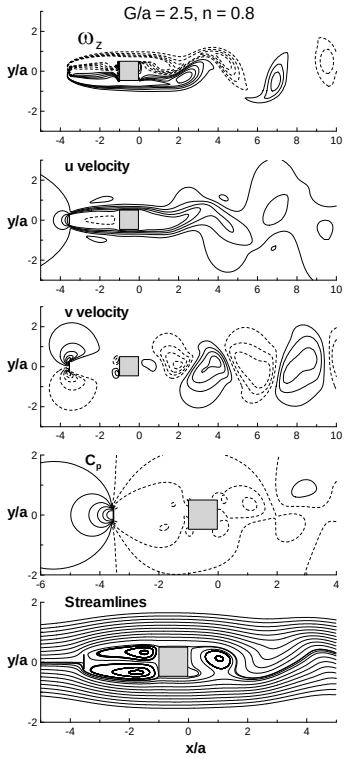

Fig. 2: Instantaneous flow visualization for different parameters: ω_z, u, v, C_p and streamlines at G/a = 2.5 and n = 1.2.

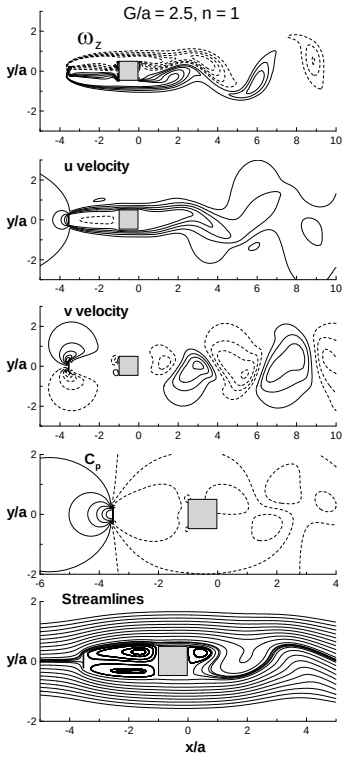

Fig. 3: Instantaneous flow visualization at G/a = 2.5 and n = 1. For detail refer Fig. 2.

For all cases due to the presence of an upstream vertical plate, the pressure at the front stagnation point of the cylinder reduces drastically. This can be attributed to a non-uniform flow field with negative pressure and flow separated velocity comes in contact with the cylinder front side. This effect also decays the size of negative pressure zone behind the cylinder which ultimately helps to reduce the drag forces. As pseudoplastic fluid (n = 0.8) is also termed as shear-thinning fluid, it is observed from Fig. 2 that the stretching of shear layers of the cylinder is quite less in this case and a proper Kármán vortex shedding is observed from x/a = 4 onwards.

As n increases to n = 1 (Fig. 3) for Newtonian fluid, the stretching of shear layers also increases and shedding of vortices start slightly away as compared to n = 0.8 case. This difference becomes more prominent in Fig. 4 (n = 1.2, dilatant or shear thickening fluid), where the shear layers are stretched up to x/a = 8. This difference in flow structures can be attributed to the diverse nature of fluid rheology.

The instantaneous u velocity contours at G/a = 2.5 (Figs. 2 - 4) illustrate that due to viscous effect (as it is generated from no-slip boundary condition) streamwise velocity reduces close to the splitter plate and cylinder. The negative u contour in between the plate and cylinder create a big separation region.

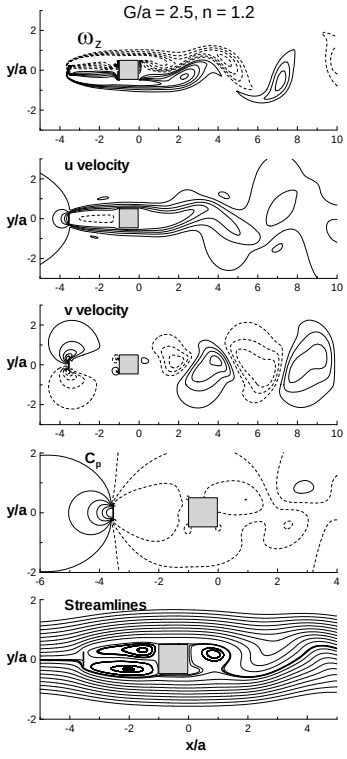

Fig. 4: Instantaneous flow visualization at G/a = 2.5 and n = 1.2. For detail refer Fig. 2.

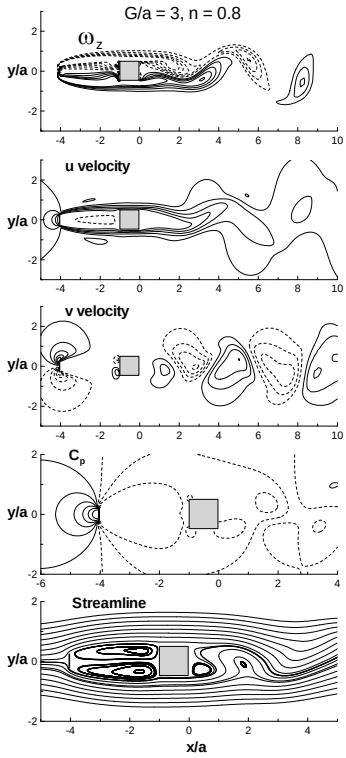

Fig. 5: Instantaneous flow visualization at *G*/*a* = 3 and *n* = 0.8. For detail refer Fig. 2.

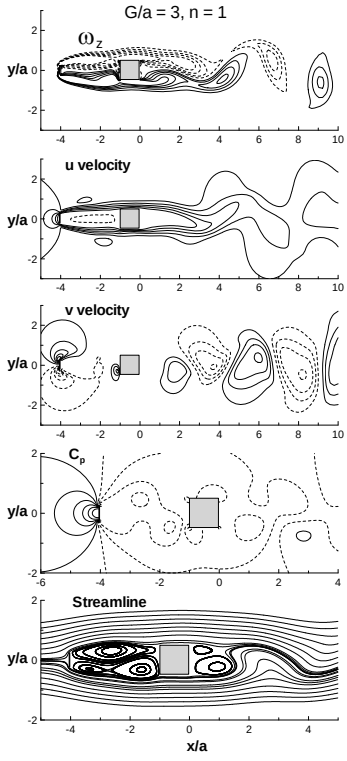

Fig. 6: Instantaneous flow visualization at *G*/*a* = 3 and *n* = 1. For detail refer Fig. 2.

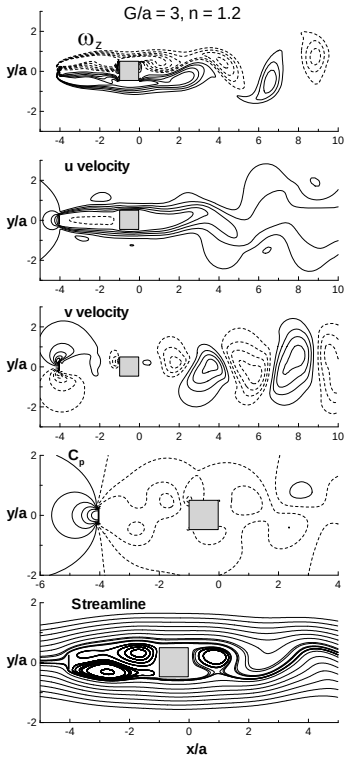

Fig. 7: Instantaneous flow visualization at *G*/*a* = 3 and *n* = 0.8. For detail refer Fig. 2.

The positive and negative contours of *v*- velocity are the mirror reflection with respect to the splitter plate center line just before the flow strikes the plate (at *G*/*a* = 2.5, Figs. 2 - 4). Downstream of the cylinder, the continuous appearance of negative and positive rolls of *v*-velocity contours can be attributed to the presence of Kármán Vortex Street in the flow field.

As the flow field first strikes the vertically placed splitter plate, the positive pressure zone occurs upstream of the plate (from instantaneous C_p contours). In the downstream of the plate, pressure field remains negative and the square cylinder is completely immersed in this negative zone. This change the flow behavior of shear layers from the square cylinder as the C_p value becomes negative at the front stagnation point of the cylinder. The wake width in the downstream of plate is marginally increased with the increase of power index *n*.

No major difference in instantaneous contours of flow variables is observed with the change of gap between plate and cylinder (*G*/*a* = 3, Figs. 5 - 7).

The lift and drag coefficients ($C_L = \frac{F_L}{\frac{1}{2}\rho U_\infty^2 a}, C_D = \frac{F_D}{\frac{1}{2}\rho U_\infty^2 a}$; where, F_L and F_D are the lift and drag forces respectively) along with mean back pressure coefficient ($C_{pb} = \frac{P_\infty - P_b}{\frac{1}{2}\rho U_\infty^2}$) and bubble recirculation length (L_r/a) values are enlisted in Table 1 for all cases.

Table 1: Variation of fluid forces

Case	Cylinder					
	$C_{L_{max}}$	$C_{L_{min}}$	$\overline{C_L}$	$\overline{C_D}$	$\overline{C_{pb}}$	L_r/a
G/a=2.5, n = 0.8	0.051	-0.051	0	0.182	-0.374	1.697
G/a=2.5, n = 1	0.065	-0.065	0	0.261	-0.375	2.072
G/a=2.5, n = 1.2	0.069	-0.069	0	0.261	-0.376	2.179
G/a=3, n = 0.8	0.024	-0.024	0	0.178	-0.338	1.735
G/a=3, n = 1	0.268	-0.270	0	0.260	-0.323	2.003
G/a=3, n = 1.2	0.312	-0.312	0	0.257	-0.329	2.326

The mean lift coefficient ($\overline{C_L}$) remains zero for the cylinder signifies no changes in mean lift coefficient as compared to an isolated cylinder. On the other hand, the mean drag coefficient ($\overline{C_D}$) for pseudoplastic (n = 0.8) fluid flow is quite low as compared to Newtonian (n = 1) and dilatant flow (n = 1.2). From the variation of maximum and minimum values of C_L it can be concluded that the magnitude of C_L fluctuation increases with the high value of n. The negative values of $\overline{C_{pb}}$ can be attributed to the negative pressure behind the cylinder. The high magnitude of $\overline{C_{pb}}$ is due to the fact that in all cases the cylinder is completely immersed in the negative pressure zone. The lowest value of L_r/a at n = 0.8 and G/a = 2.5 is associated with low separation region and early vortex formation.

For a better understanding of the flow field behind a square cylinder in the presence of an upstream vertically placed splitter plate, the time averaged (mean) vorticity contours ($\overline{\omega_z}$) are also included in the present work. As Re belongs to laminar periodic vortex shedding regime (Re = 150), the time averaged data is taken by averaging the flow variables for 5 consecutive time periods.

Fig. 8 illustrates $\overline{\omega_Z}$ contours at G/a = 3 for different fluid flow (n = 0.8, 1 and 1.2). Here, negative contours are shown by dashed lines and solid lines shows the positive contours. It has been observed from the figures that as the value of n increases from n = 0.8 to 1, the magnitude of vorticity in the flow field increase. Also the upper and lower vortices are symmetrical in size with respect to the axis passing through cylinder center line. Downstream of the cylinder vortices diverge from the center axis.

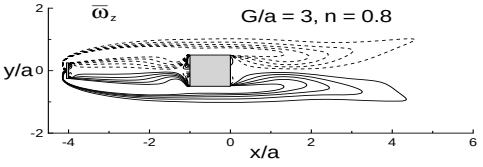

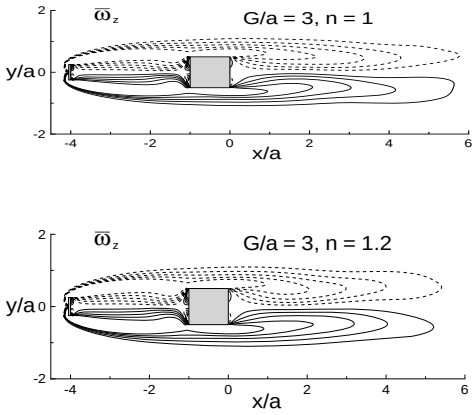

Fig. 8: Time-averaged vorticity at G/a = 3 for n = 0.8, 1 and 1.2.

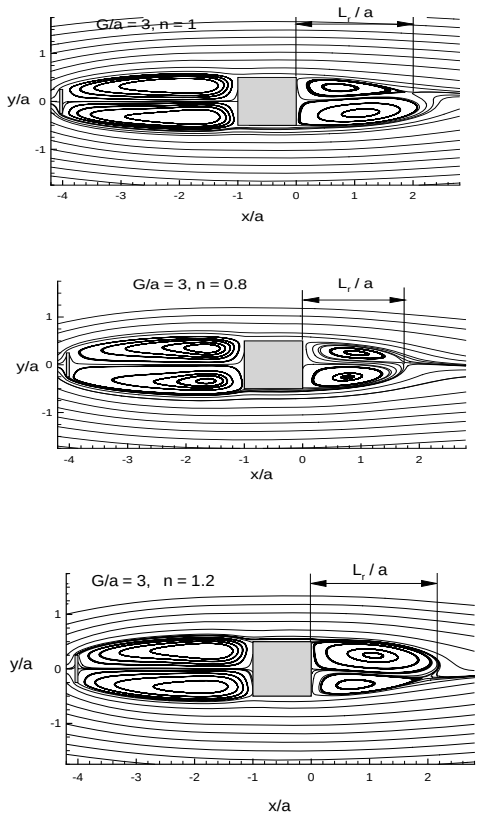

Fig. 9: Time-averaged streamlines at G/a = 3 for n = 0.8, 1 and 1.2.

In Fig. 9 a set of time-averaged streamlines are drawn with equal space interval to understand the mean flow field. The streamline plot helps us to calculate the length of the separation bubble behind the cylinder. These mean streamlines are obtained from mean velocity field $\overline{u}$ and $\overline{v}$. In the present case two separation regions are obtained, the first one is in between the splitter plate and square cylinder and next one just

after the cylinder. The second separation bubble after the cylinder is the main reason to delay the vortex formation from the cylinder. The non-dimensional length of separation bubble which is represented by L_r/a as shown in Fig. 9 is tabulated in Table 1 for varying gap ratios and varying values of n. The comparison of these values illustrates the increase of separation bubble region for any particular gap ratio with the increase in value of n.

4. CONCLUSION

Vortex control behind a square cylinder is numerically solved at Re = 150 using an upstream splitter plate placed vertically. Three different fluids are considered for this purpose: Newtonian (n = 1), pseudoplastic (n = 0.8) and dilatant (n = 1.2). Two different gap ratios (G/a = 2.5, 3) are considered following Malekzadeh and Sohankar (2012) who simulated the similar problem for Newtonian flow at Re = 50 to 200.

Both the instantaneous and mean flow fields are illustrated in the present result with the help of several flow variables. Following conclusions are made from the obtained results:

1. From instantaneous flow field it can be concluded that for Newtonian flow, stretching of shear layers occur behind the cylinder which delayed the vortex formation.
2. For pseudoplastic flow, due to shear thinning effect the shear stress in the wake region reduced which simultaneously reduced the stretching of shear layers and therefore an early vortex roll-up is observed.
3. In case of dilatant flow, due to its shear thickening effect, the stretching of shear layer is more as compared to Newtonian flow which further delayed the formation of vortices.
4. Instantaneous C_p contours for all cases illustrated a negative pressure zone behind the splitter plate which completely submerged the downstream cylinder. Therefore, the front stagnation pressure of the cylinder becomes negative which ultimately delayed the vortex formation as compared to the unbounded cylinder.
5. Two separation regions are found for u contours (for all cases), where the first one lies in between the plate and cylinder and the second one occurs just after the cylinder.
6. From the tabulated values of $\overline{C_d}$, it has been observed that $\overline{C_d}$ is less at G/a = 3 as compared to G/a = 2.5 considering different n. This result is consistent with the finding of Malekzadeh and Sohankar, who concluded G/a = 3 is the critical gap ratio (minimum $\overline{C_d}$) for the similar flow geometry at Re = 160.
7. The minimum value of $\overline{C_d}$ is obtained for pseudoplastic flow whereas it becomes maximum for dilatant flow.
8. The mean flow field of all variables shows symmetric contours with respect to cylinder centre line.

REFERENCES

[1] Fransson, J. H. M., Konieczny, P., and Alfredsson, P. H., "Flow around a porous cylinder subject to continuous suction or blowing", *Journal of Fluids and Structures*, 19, 2004, pp. 1031–1048.

[2] Darekar, R. M., and Sherwin, S. J., "Flow past a bluff body with a wavy stagnation face", *Journal of Fluids and Structures*, 15, 2001, pp. 587–596.

[3] Eckelmann, H., Graham, J. M. R., and Huerre, P., Monkewitz, P. A., "Bluff Body Wakes, Dynamics and Instabilities", *I.U.T.A.M. Symposium Gottingen, Springer, Germany*, 1992, pp. 227-240.

[4] Fiedler, H. E., and Fernholz, H. H., "On management and control of turbulent shear flows," *Progress in Aerospace Science.*, 27, 1990, pp. 305-387.

[5] Srivastava, S., and Sarkar, S., "Wake interaction of a square cylinder with a splitter plate boundary layer at a low Reynolds number*", AJK2015*-FED, Seoul, 2015, AJKFluids2015-01793 (6 pages).

[6] Jain, S., Sharma, S., and Sarkar, S., "Low Reynolds number flow over a square cylinder in vicinity of a downstream splitter plate", Journal of Material Science and Mechanical Engineering, 13(2), 2015, pp. 77-81.

[7] Malekzadeh, S., and Sohankar, A., "Reduction of fluid forces and heat transfer on a square cylinder in a laminar flow regime using a control plate", *International Journal of Heat and Fluid Flow*, 34, 2012, pp. 15–27.

[8] Chilcott, M. D., and Rallison, J. M., "Creeping flow of dilute polymer solutions past cylinders and spheres", *Journal of non-Newtonian Fluid Mechanics*, 29, 1988, pp. 381–432.

[9] Kato, H., and Mizuno, Y., "An experimental investigation of viscoelastic flow past a circular cylinder", *Bull. JSME*, 36, 1983, pp. 529–536.